

The emission line presented here could have several plausible origins other than Lyman- α , including non-random detector noise, night-sky residuals, or another astrophysical emission line at lower redshift. Here we discuss the reduction methods, and provide several tests of the detection, to demonstrate why it is Lyman-alpha emission.

S1 Observations and Data Reduction

We used SINFONI³¹ on UT4 of the VLT to obtain deep, 3-dimensional spectroscopy of UDFy-38135539. We observed UDFy-38135539 in the J band, which covers the expected wavelength of Ly α at a redshift $z \sim 8.5$, the redshift determined from the multi-wavelength photometry available for this source³². We observed for 16 hrs, granted as Director's Discretionary Time (program ID 283.A-5058), and obtained a total of 53400 seconds of integration time on the source. Individual exposure times were 600s, and we adopted a dither pattern where the source remained in the field of view for all exposures. Observing faint, high-redshift galaxies requires a high accuracy in the pointing, better than 1". We therefore defined our pointing by acquiring a star at about 1.5' from the position of UDFy-38135539³² at the beginning of each Observing Block (a sequence of 5-6 individual exposures with a total length of 1 hr). At the end of each Observing Block we observed a nearby star of known J-band magnitude and spectral type at a similar airmass. Flux scales were obtained from these stars, and we also used the size of the point spread function of these stars to monitor the seeing.

An additional uncertainty can arise in the calibration due to both the variation in the atmospheric absorption at the wavelength of the line and to the crudeness of the flux calibration. The depth of absorption in the spectral region near the line is significant, $\approx 10\text{-}30\%$, and is variable depending on the amount of water vapour in the atmosphere and the telescope elevation during which the observations were taken. The data and standard stars are taken at somewhat different times and air masses, adding additional uncertainty. Spectrophotometric calibration in the near-infrared is not very accurate. There are no generally available spectrophotometric standards as in the optical and the calibration star is used to simultaneously provide flux calibration and to remove the effects of atmospheric absorption. The crudeness of the calibration probably induces an additional uncertainty of 20-30% and changes in the atmospheric absorption between the observations of the source and calibration star can introduce systematic uncertainties of about the same order. This additional uncertainty does not influence the significance of the detection, as the measurement of the noise and the line flux are affected by the same systematic uncertainties, but it does influence the accuracy of the estimate of the line flux. Systematic uncertainties in the absolute flux measurement are therefore of-order 30-40%.

The instrumental resolution was measured from the widths of night sky lines extracted from a SINFONI cube near the wavelength of the line, and the error estimates are based on a Monte-Carlo simulation of the data with a Gaussian line profile and the noise characteristics of the region near the line. To determine the instrumental resolution, we used a data cube obtained in exactly the same manner as the science data with the only difference being that we did not subtract the night sky. The spectral resolution was measured to be 190 km s^{-1} or $R = \lambda / \Delta\lambda = 1580$ at $\lambda \sim 1.16 \mu\text{m}$.

The data were reduced using our own data reduction software based on IRAF³³. These routines have been tested and used extensively and have been discussed extensively in previous articles^{34,35,36,37}. A study similar to this one has been attempted previously³⁸.

ID	λ_{obs}	redshift	FWHM	Flux
Ly α	11615.6 \pm 2.4	8.5549 \pm 0.0002	9.2 \pm 1.2	6.1 \pm 1.0

Table 1: Emission-line properties measured from our SINFONI data of UDFy-38135539. Column (1) – Line ID. Column (2) – observed wavelength. Column (3) – Redshift assuming the line is Ly α at 1215.67 \AA . Column (4) – Measured full width at half maximum (FWHM) in units of \AA . The line is unresolved. Column (5) – Line flux in units of $10^{-18} \text{ erg cm}^{-2} \text{ s}^{-1}$. The uncertainty in the line flux is derived from repeated realisation of the line given the noise in the data set. There is a systematic uncertainty of the flux of 30-40% which is not included in the estimate given.

S2 The Nature of the Line

An obvious concern in searching for faint line emission from galaxies at the highest redshifts is that the detection is spurious. This is particularly worrisome for near infrared observations. Near-infrared detectors have pixels that do not behave linearly with exposure and/or have a significantly different response from the vast majority of pixels. In addition, the line and continuum emission from the sky emission has structure and is also variable. These effects result in reduced data that do not have strictly Gaussian random noise. These effects can be largely, but not entirely corrected for during the data reduction. Because of this, it is important to make a number of comparisons between the properties of any putative emission line and those expected for a real signal.

To show that the line is not an instrumental artefact, we have made several tests that an astrophysical line must meet at a minimum to be considered real.

S2.1 Characteristics of the Line

The line in the integrated spectrum has a width that is slightly larger than the instrumental resolution. The characteristics of the line detected in our cube are given in Table 1. While we would expect the Ly α profile to be intrinsically asymmetric due to the absorption on the blue side of the profile due to neutral Hydrogen, the observed line is not resolved and thus has a Gaussian profile. Observations of Lyman- α emitting galaxies at redshifts around 5 also show symmetric profiles when they are approximately unresolved, even with much higher signal-to-noise than 6³⁹. The faintness of the signal and low signal-to-noise makes it impossible to detect the faint, and possibly non-Gaussian wings often observed in Ly α emitting galaxies.

The extent of the line image is $0.6'' \times 0.7''$, similar to the size of the seeing disk which results from atmospheric turbulence. The WFC3 image³² shows that the source has an intrinsic size in the continuum of $0.3''$. If the emission line region of the source is not larger than the continuum source by about a factor of 2, it would be unresolved in our data as observed.

The line is found in a region of the night sky that is relatively free of bright night-sky lines. Night-sky line residuals, due to mechanical instabilities of the instrument leading to small (fractions of a pixel) wavelength shifts, can lead to features that may be mistaken for real emission lines. The brightest of these spurious features arise in a part of the data cube that is near the edge of the slitlets of the slicer. In Fig. 1 of the main article, the night sky line residuals are more prominent near the periphery of the spectrum. The candidate Lyman alpha emitter is in a region of the cube that is unaffected by the edges of the slitlets.

The line emission is within $0.4''$ of the expected position of the source in our data cube, and within about one half of the size of the point spread function. Due to the low signal-to-noise of the detection itself, uncertainties in the relative astrometric position of the offset star and target, and inaccuracies in the telescope offset, imply that the offset we observe in our cube is consistent with the position of the source.

S2.2 Random or Correlated Noise?

All of these suggest at a minimum that the emission line is consistent with being of astrophysical origin from the targeted source. Even though it appears that this is likely to be an emission line from a source, it could also be that this is a rare noise spike in the data that coincidentally happens to have characteristics expected for an astrophysical source. We will now illustrate that the line with the properties we have estimated is also rare, rare enough not to be associable with random or correlated detector noise.

In our three-dimensional data cube we estimate that there are approximately 500,000 pixels where we expect night-sky line residuals that are similar to those in the area covered by the source (and which are contained in all exposures). We used a simple Monte Carlo approach to investigate how many of these pixels could produce a spurious noise signal similar to the actual signal that we have observed.

We randomly selected a spatial position covered by the data cube and extracted the 25 one-dimensional spectra centred on that position (in a 5 by 5 spatial pixel region, specifically chosen to be approximately the size of one seeing disk). We then randomly selected a wavelength within the region covered by those spectra and, for each spectrum, fitted a Gaussian line profile centred at that wavelength. The width of the fitted Gaussian was constrained to be between the spectral resolution and 400 km s^{-1} and its total flux was allowed to vary between 3 and 90 times the noise level. We then determined how many of the 25 spectra had acceptable fits comparable to the detected feature.

This procedure was repeated 25000 times and on 301 occasions (1.2%) resulted in reasonable fits for one or more of the 25 extracted spectra (see Fig. 1). The maximum number of spectra with acceptable fits in any one trial was eleven, found in a single trial. There was not a single instance of all 25 spectra resulting in acceptable fits, as there was for the detected feature. Given the statistics shown in Figure 1, the probability of generating such a feature purely from the noise characteristics of the data cube is at best one in 25000 (a confidence level of $> 99.99\%$), and likely considerably lower.

S2.3 A Spurious Line: Negative Line Image

There are several other ways to argue that the line is not likely to be spurious. We searched for the negative images of the line which are a by-product of our observing strategy, and allow for a particularly powerful test of the astrophysical origin of our signal. We adopted a dither strategy where the source is within the field of view at all times, but falls into different parts of the detector in subsequent individual exposures. This means that we can use one object frame to subtract the sky from another, and the presence of the source in each of these frames implies that we produce a characteristic negative signal in each individual sky-subtracted frame, where we subtract the source from an empty part of the sky. We will refer to this negative signal as the “shadow”. Identifying the shadow is a particularly powerful test, since the shadow arises from a different part of the detector, sharing only half the pixels with the source in each individual exposure. From our experience with integral-field spectroscopy with this instrument of over a 100 faint galaxies, we are not aware of any data cube where a shadow would have been produced by an instrumental artefact.

Since the shadow does not fall in the same region of the detector for all dithers, and because the line is so faint, we reconstructed a dedicated “shadow cube” from the individual frames. We calculate the expected position of the shadow in each individual exposure from the measured target position. We then shift the individual cubes such that all shadows fall on the same position and combine the individual exposures to obtain a shadow cube, where the residual of the target falls at the same position as the galaxy in the original combined cube (Fig. 2). The shadow line is clearly seen at the wavelength of the detected line (Gaussian line profile above the spectrum), and with a similar width and flux.

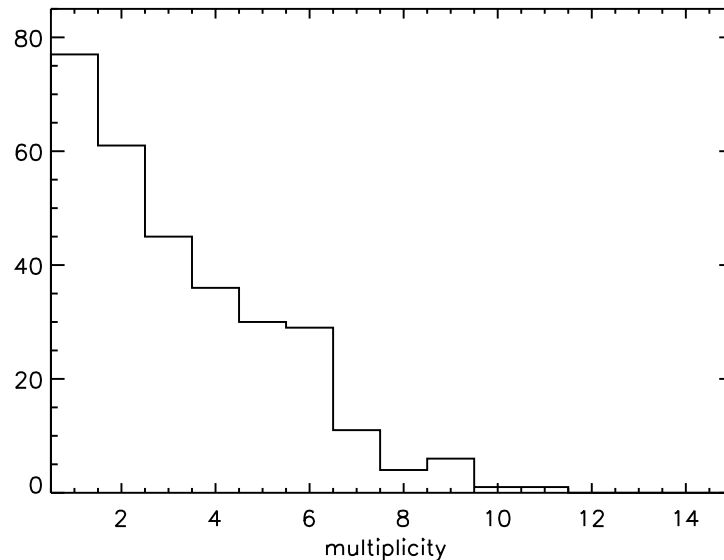


Figure 1: The “multiplicity” distribution. The multiplicity is the number of pixels that can adequately be fit with similar fit parameters within a box corresponding to the size of the seeing disk (5×5 pixels), surrounding a randomly chosen pixel in a region containing no signal from and have noise characteristics similar to that of the region around the detected line emitter. The detected line emitter has a multiplicity of 25, whereas in the noise has multiplicities ≤ 11 . Having found a multiplicity of 11 in 1 trial of 25,000, we can rule out larger multiplicities due to noise at a confidence level $>99.996\%$.

We also evaluated the individual frames to infer whether the candidate emission line may be dominated by non-Gaussian noise originating from individual frames. We followed two approaches. We constructed two cubes each containing half of the frames. For Gaussian noise we expect to find a signal-to-noise ratio lower by $\sqrt{2}$ in each subset, giving $\text{SNR} \sim 4.6\sigma$. We extracted integrated spectra at the same position and with the same apertures as for the full data set, and measured the signal-to-noise ratio of each line. We find signal-to-noise ratios of 4.3σ and 3.5σ for each subset, respectively. Given that the faintness of the detection alone makes each estimate accurate only within $\sim 25\%$ this is fully consistent with what is expected for half of the full data set.

To further evaluate whether the signal may be dominated by strongly deviant pixels in individual frames, we also extracted line images for each individual, fully reduced data cube, by collapsing over the wavelength range near the wavelength of our line detection. In total we cover a range of 30\AA ($3 \times$ the full width at half maximum (FWHM) of the line) to be conservative. (By conservative, we mean that we took a spectral range much larger than necessary to extract the signal and therefore will possibly include additional sources of non-random noise). We then inspected each line image individually, in order to identify frames which were affected by bad pixels and/or night-sky line residuals at the position of the source. We found that 20 of the frames *could* be contaminated. However, since the line image covers a range of 30\AA , which includes a faint night sky line residual slightly red-ward of the source, this does not imply necessarily that the line itself is affected. We combined all 20 of the contaminated frames (which had non-Gaussian noise near the position of the source) and also the remaining 69 frames that were not so affected (i.e., where the noise was better behaved and approximately Gaussian). We found a strong, narrow (FWHM ~ 1.3 spectral pixels)

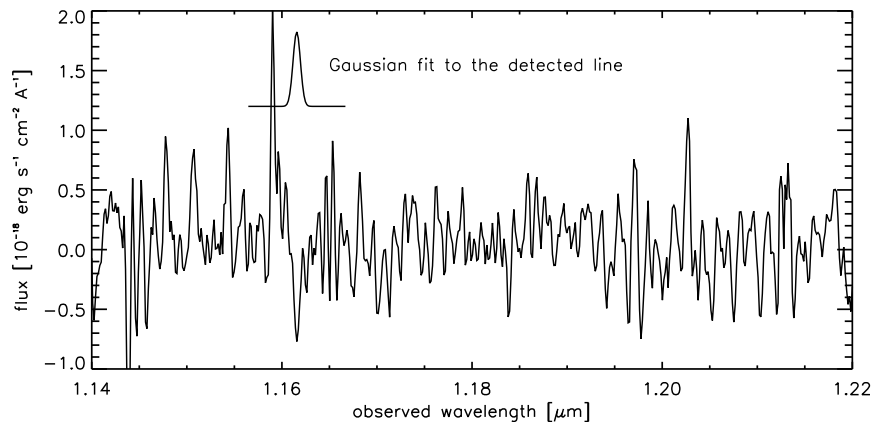


Figure 2: The integrated spectrum of the “shadow” in the data set. Our strategy for subtracting the sky and combining the data set produces a negative residual due to the presence of the source in all sky-subtracted frames. These shadow shares all of the exposures at the position of the source, but a completely different set of pixels in the “off” position compared to the positive image. The Gaussian profile marks the fit of the Lyman- α emission line and the negative residual is clearly visible.

spike in the cube constructed using the frames that were contaminated, but at the wavelength of a night-sky line, and recovered a faint line consistent with that found in the full data set in the combined cube of individual frames that were not contaminated. Within the larger uncertainties, this cube of uncontaminated frames also produced a line with a flux consistent with that found when using the full data set. We thus conclude that the frames with strongly non-Gaussian noise do not have a significant impact on our line measurement in the full cube.

S3 Other Possible Sources of Line Emission

Having shown that instrumental effects are unlikely to cause the observed emission line, could it be a line due to a source at lower redshift that is not Lyman- α ? The very red colour and lack of detection in the optical ($B_{435} < 29.8$, $V_{606} < 30.2$, $i_{775} < 29.8$, $z_{850} < 29.1$ all $2\text{-}\sigma$ limits)⁴⁰ makes it highly unlikely that UDFy-38135539 could be an emission line galaxy at lower redshift^{32,40}. The best fit redshift for the photometry is $z=8.45$ with an acceptable range of $z=7.75\text{--}8.85$. There is also a shallow (reduced $\chi^2_\nu = 3$) secondary minimum in the probability distribution at $z=1.60\text{--}2.15$, which could be caused by a large spectral break at 4000\AA in the rest-frame of the galaxy⁴⁰.

The much fainter and more stable backgrounds of the WFC3 on board the *Hubble Space Telescope* compared to ground-based near-infrared imagers make the photometry particularly robust. However, additional systematic uncertainties are possible, for example line contamination in the filter bandpass used to discover the source. Our measured line flux, taken at face value, would lower the intrinsic J_{125} magnitude from $J=28.41\pm 0.24$ to $J_{125}^{corr}=29.7\pm 0.3$, implying a bluer intrinsic continuum J-Y colour, $Y_{105}\text{--}J_{125}^{corr} > 1.0\pm 0.3$ ($1\text{-}\sigma$), and a lower redshift is possible. This illustrates the importance of emission-line measurements for candidate Lyman-break galaxies at the highest redshifts, and makes

it worthwhile to specifically test all alternative redshifts that may be implied by the line detection.

The only other plausible line identifications at lower redshifts are the generally bright lines from galaxies of $H\alpha$ at 656.3nm, which would imply a redshift of $z=0.77$, [OIII] at 500.7nm, which would imply a redshift of $z=1.32$, and the [OII] doublet at 372.6 and 372.9 nm, which would imply a redshift of $z=2.12$. Given the secondary minimum in the photometric redshift distribution around $z\sim 2^{40}$, we must make detailed tests of the possibility that the detected line could be [OII] at $z=2.12$. For illustration purposes only, we have added an artificial doublet line profile to our data set after subtracting off our best fit profile from the line (Fig. 3). The figure shows that any [OII] doublet emission should be both resolved and wider than the current best fit single line. To go beyond this illustration and to show statistically that the [OII] doublet is inconsistent with the properties of the line, we carried out a simple Monte-Carlo simulation. For this we generated 10^6 artificial data sets with the noise characteristics of our data cube, and added two delta functions separated by $2.8(1+z_{[OII]})\text{\AA}$ which were then convolved with two Gaussian profiles with the resolution of our data. We assumed a line ratio $R_{3726/3729} = 1$. In a vast majority of the cases ($\sim 99\%$) we see a resolved doublet, and in all cases, a width of the doublet that is significantly greater than that of the detected line (with an average width of $15\pm 1.2\text{\AA}$). Similar results are found when testing a few other plausible ratios of the two [OII] components. We can therefore rule out that the line is [OII] $\lambda\lambda 372.6, 372.9$ at $z=2.12$ at a level greater than 99.9% or $3\text{-}\sigma$ because it produces a line that is clearly broader than that measured.

From the photometry and the line flux, the observed equivalent width of the line is about 1900\AA . All hypotheses other than $Ly\alpha$ at $z=8.55$ also imply implausibly high equivalent widths for optical lines of ≈ 600 to $1,100\text{\AA}$, which are not observed in the integrated spectra of local galaxies⁴¹ or even the majority of the rare photometrically selected galaxies that have extremely high equivalent widths⁴². Even if we include a systematic uncertainty in the flux of several tens of percent, up to 40%, this would still be highly implausible. We therefore conclude that the line is indeed most likely $Ly\text{-}\alpha$ at $z=8.55$.

We finally conclude that the line detected is not spurious, is inconsistent with an instrumental artefact, and is inconsistent with being an emission line at lower redshift.

References

- [31] Bonnet, H., et al., First light of SINFONI at the VLT, *The Messenger*, **117**, 17-24, (2004).
- [32] Bouwens, R. J., Illingworth, G. D., Oesch, P. A., Stiavelli, M., van Dokkum, P., Trenti, M., Magee, D., Labbé, I., Franx, M., Carollo, C. M., & Gonzalez, V., Discovery of $z\sim 8$ Galaxies in the Hubble Ultra Deep Field from Ultra-Deep WFC3/IR Observations, *Astrophysical Journal*, **709**, L133-L137, (2010).
- [33] Tody, D. 1993, in *Astronomical Data Analysis Software and Systems II*, ed. R. J. Hanisch, R. J. V. Brissenden, & J. Barnes (San Francisco: ASP), 173
- [34] Nesvadba, N. P. H., Lehnert, M. D., De Breuck, C., Gilbert, A. M., & van Breugel, W., Evidence for powerful AGN winds at high redshift: dynamics of galactic outflows in radio galaxies during the ‘‘Quasar Era’’, *Astronomy and Astrophysics*, **491**, 407-424, (2008).
- [35] Nesvadba, N. P. H., Lehnert, M. D., Davies, R. I., Verma, A., & Eisenhauer, F., Integral-field spectroscopy of a Lyman-break galaxy at $z = 3.2$: evidence for merging, *Astronomy and Astrophysics*, **479**, 67-73, (2008).
- [36] Nesvadba, N. P. H., Lehnert, M. D., Genzel, R., Eisenhauer, F., Baker, A. J., Seitz, S., Davies, R., Lutz, D., Tacconi, L., Tecza, M., Bender, R., & Abuter, R., Intense Star Formation and

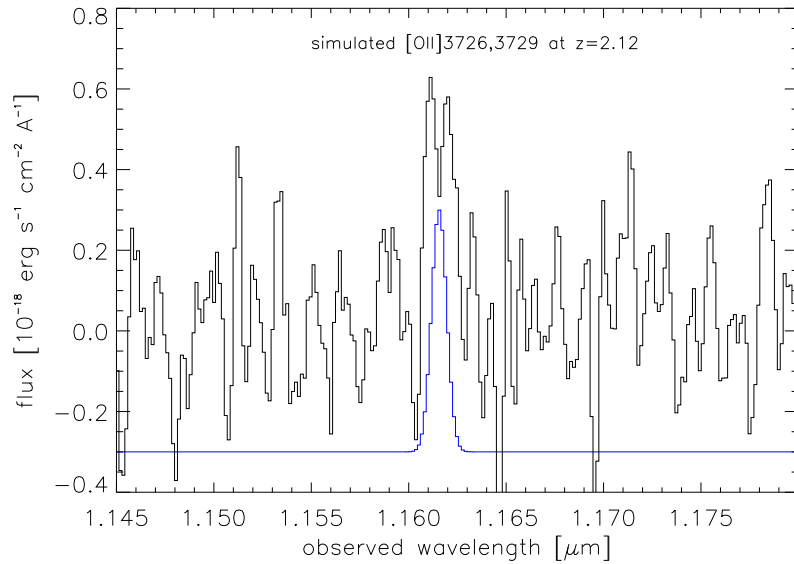


Figure 3: An alternative identification for the line as arising from the doublet of singly ionised Oxygen. To illustrate that it is unlikely that the identified line is consistent with being [OII] $\lambda\lambda$ 372.6,372.9 at lower redshift we subtracted our best fit Gaussian profile for the data cube to remove the emission from the source. This produces a line-free spectrum with the noise characteristics for our data cube in the region of and near the wavelength of the line. At line centre, we added two delta functions separated by $2.8(1+z_{[OII]})\text{\AA}$ which have been convolved with a Gaussian profile. This profile has a width that is exactly the same as the spectral resolution of our data. For this illustration we assumed a line ratio $R_{3726/3729} = 1$ and a redshift of 2.12. This redshift corresponds approximately to the secondary minimum in the redshift probability distribution derived from the WFC3 photometry⁴⁰. The blue line shows the Gaussian fit to our data shifted along the ordinate for comparison. Clearly the doublet would be resolved spectrally and overall be broader than the detected emission line even at the low signal-to-noise of our detection.

- Feedback at High Redshift: Spatially Resolved Properties of the $z = 2.6$ Submillimeter Galaxy SMM J14011+0252, *Astrophysical Journal*, **657**, 725-737, (2007).
- [37] Lehnert, M. D., Nesvadba, N. P. H., Tiran, L. L., Matteo, P. D., van Driel, W., Douglas, L. S., Chemin, L., & Bournaud, F., Physical Conditions in the Interstellar Medium of Intensely Star-Forming Galaxies at Redshift 2, *Astrophysical Journal*, **699**, 1660-1678, (2009).
- [38] Richard, J., Stark, D. P., Ellis, R. S., George, M. R., Egami, E., Kneib, J.-P., & Smith, G. P., A Hubble and Spitzer Space Telescope Survey for Gravitationally Lensed Galaxies: Further Evidence for a Significant Population of Low-Luminosity Galaxies beyond $z=7$, *Astrophysical Journal*, **685**, 705-724, (2008).
- [39] Douglas, L. S., Bremer, M. N., Lehnert, M. D., Stanway, E. R., & Milvang-Jensen, B., Spectroscopy of $z\sim 5$ Lyman Break Galaxies in the ESO Remote Galaxy Survey, *Monthly Notices of the Royal Astronomical Society*, accepted (2010).
- [40] McLure, R. J., Dunlop, J. S., Cirasuolo, M., Koekemoer, A. M., Sabbi, E., Stark, D. P., Targett, T. A., & Ellis, R. S., Galaxies at $z = 6-9$ from the WFC3/IR imaging of the Hubble Ultra Deep Field, *Monthly Notices of the Royal Astronomical Society*, **403**, 960-983, (2010).
- [41] Kennicutt, R. C., Jr., The integrated spectra of nearby galaxies - General properties and emission-line spectra, *Astrophysical Journal*, **388**, 310-327, (1992).
- [42] Cardamone, C., Schawinski, K., Sarzi, M., Bamford, S. P., Bennert, N., Urry, C. M., Lintott, C., Keel, W. C., Parejko, J., Nichol, R. C., Thomas, D., Andreescu, D., Murray, P., Raddick, M. J., Slosar, A., Szalay, A., & Vandenberg, J., Galaxy Zoo Green Peas: discovery of a class of compact extremely star-forming galaxies, *Monthly Notices of the Royal Astronomical Society*, **399**, 1191-1205, (2009).